Mon. Not. R. Astron. Soc. **000**, 1–16 (1999) Printed 27 August 1999 (MN LaTeX style file v1.4)

RXTE observations of Galactic microquasar XTE J1748–288 during its 1998 outburst

M. G. Revnivtsev[1,2], S. P. Trudolyubov [1,2] and K. N. Borozdin [3,1]
[1] *Space Research Institute, RAS, Profsoyuznaya 84/32, 117810 Moscow, Russia*
[2] *Max-Planck-Institut für Astrophysik, Karl-Schwarzschild-Str. 1, 85740 Garching bei Munchen, Germany*
[3] *Los Alamos National Laboratory, Los Alamos, 87545 New Mexico, USA*

Accepted Received in original form ??

ABSTRACT

We present an analysis of the *RXTE* observations of the recently discovered Galactic microquasar XTE J1748–288 during its 1998 outburst. General spectral and temporal properties of the source and their evolution were very typical for the Galactic black hole candidates (BHC) and, in particular, black hole X-ray Novae.

The spectral evolution of the source during the outburst can be considered a sequence of qualitatively distinct states. During the first observations, corresponding to the maximum of X-ray flux, the spectrum of the source consisted of a dominating hard power law component and a soft thermal component, which can be described by the model of multicolor disk emission. The hard component contributed $\geq$80% to the X-ray luminosity in the 3-25 keV energy band. Overall two-component spectral shape is an attribute of *very high* state (VHS) observed previously in BHC, but the domination of hard component is unusual. Later on, as the X-ray source faded, its energy spectrum qualitatively changed, showing *high* (HS) and then *low* (LS) states, both typical for black hole binaries.

As the energy spectrum changed, the fast variability also evolved dramatically. Initially the power density spectrum was formed by a dominating band-limited noise component, QPO features at 20-30 Hz and at $\sim$0.5 Hz, and a very low frequency noise component. After a significant decrease of the contribution of the hard spectral component the amplitude of the fractional variability decreased by an order of magnitude and the PDS spectrum adopted a power-law shape with a broad QPO peak around 0.03 Hz. When the system switched to the LS, the PDS shape changed again and the QPOs have not been detected since.

When the source was observed in VHS, a clear correlation between QPO parameters and X-ray flux was seen. Such a correlation gives an insight into our understanding of the accretion process in X-ray black hole binaries.

Key words: black hole physics – stars:binaries:general – stars:individual:XTE J1748–288 – stars:novae – X-rays: general

1 INTRODUCTION

The XTE J1748–288 was discovered as a new transient source on June 4, 1998 by All Sky Monitor (ASM) aboard the Rossi X-ray Timing Explorer *(RXTE)* observatory (Smith, Levine & Wood 1998). The X-ray source was localized with an accuracy of 1 arcmin in multiple scans of the region by the PCA/*RXTE* experiment (Strohmayer & Marshall 1998). Observations in the radio band by VLA revealed the presence of an unresolved radio source with a position consistent with one found by PCA: R.A.=$17^h48^m05^s.06$, Dec=$-28^\circ28'25''.8$ (equinox 2000.0, position uncertainty $0.''6$, Hjellming, Rupen & Mioduszewski 1998). Significant variability of the new radio source (Hjellming et al. 1998a; Fender & Stappers 1998) strongly supports its association with the X-ray transient. In June 14.31 radio source became extended, with a proper motion of 20-40 mas/day (Rupen, Hjellming & Mioduszewski 1998). The intrinsic velocity of the moving jet was higher than 0.93c for the distance $\geq$8 kpc derived from a 21 cm HI absorption measurement (Hjellming et al. 1998b).

Two quasi periodical oscillations (hereafter QPO) with the central frequencies $\sim$0.5 Hz and $\sim$32 Hz were

Table 1. *RXTE* observations of XTE J1748–288 in 1998

#	Obs.ID	Date, UT	Time start	PCA Exp. sec
1	30188-05-01-00[a]	04/06/98	20:05:04	16
2	30188-05-02-00[a]	05/06/98	03:03:44	64
3	30171-02-01-00	06/06/98	09:41:20	2655
4	30185-01-01-00	07/06/98	07:56:32	2944
5	..-02-00	08/06/98	06:23:28	3027
6	..-03-00	09/06/98	12:48:00	3729
7	..-04-00	10/06/98	03:38:24	7721
8	..-05-00	11/06/98	12:52:16	3439
9	..-06-00	13/06/98	12:51:28	3114
10	..-07-00	15/06/98	04:53:36	1795
11	..-08-00	18/06/98	20:55:12	2327
12	..-09-00	22/06/98	22:30:08	3210
13	..-10-00	27/06/98	11:39:28	1647
14	..-11-00	08/07/98	16:21:52	1295
15	..-12-00	13/07/98	06:44:00	2056
16	..-13-00	18/07/98	04:00:32	10585
17	..-14-00	30/07/98	09:44:48	6841
18	..-15-00	05/08/98	18:25:20	4333
19	..-16-00	13/08/98	10:17:36	1565
20	..-17-00	20/08/98	16:41:20	1704
21	..-18-00	25/08/98	03:32:00	1785
22	..-19-00	14/09/98	08:17:36	886
23	..-20-00	26/09/98	03:29:04	10287

[a] – Only the “slew” parts of these observations were public at the time of our analysis

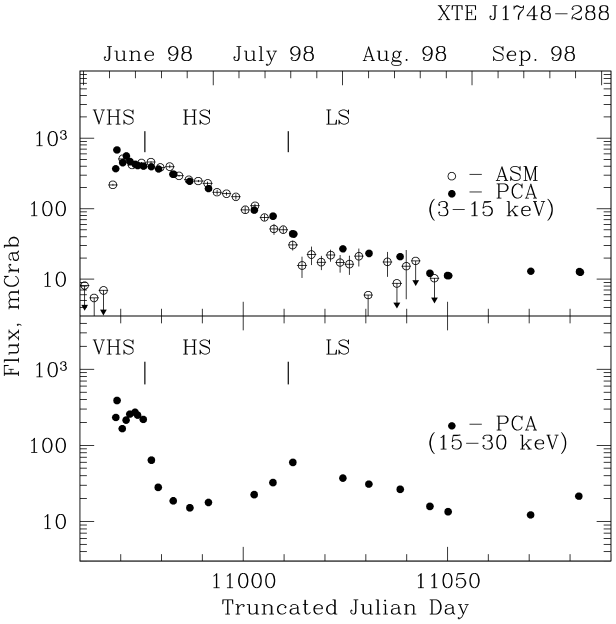

Figure 1. The light curves of XTE J1748–288 during its 1998 outburst according to the data of RXTE/ASM (2 – 12 keV energy range – upper panel, hollow circles) and PCA (3 – 15 keV energy range – upper panel, filled circles; 15 – 30 keV energy range – lower panel, filled circles).

found in the power density spectrum (PDS) of the source in the PCA observation of June 6, 1998 (Fox & Lewin 1998).

The flux from the source was above ASM/*RXTE* detection limit until August of 1998. Pointed instruments of RXTE - PCA and HEXTE - observed the source quasi evenly from June till September, obtaining a good coverage of the whole outburst. Here we present the results of a spectral and timing analysis of these RXTE observations.

2 OBSERVATIONS AND ANALYSIS

In our analysis we used all the publicly available data obtained from RXTE TOO (Target Of Opportunity) archive including 21 pointed observations and “slew” parts of two PI restricted observations. The 23 observations quasi evenly cover the 1998 outburst of the source with a total exposure of ∼ 80 ksec. The list of observations is presented in Table 1.

For data reduction we used the standard FTOOLS package. For the spectral analysis we used PCA data collected in the 3–25 keV energy range. The response matrix was constructed for every single observation using PCARMF v3.5. For the PCA background estimations we applied a Very Large Events (VLE)-based model. For some observations, where the standard VLE-based background subtraction was not good enough for our purposes, we used the activation component for background models separately (see details in the RXTE Cook Book, “Using the Latest PCABACKEST”). All spectra were dead time corrected. The analysis of the spectra of the Crab nebula confirmed that the uncertainties attributed to the response matrix do not exceed 0.5–1.0%. To account for the uncertainty in the knowledge of the spectral response, a 1 per cent systematic error was added to the statistical error in each PCA channel.

For our timing analysis we used the PCA timing modes *Binned*, *SingleBinned*, *Event* and *Good Xenon*. Background subtracted light curves from *Standard*2 mode data were used to generate the power density spectra for very low frequencies (below 10^{-2} Hz).

Unfortunately, an analysis of the HEXTE data was strongly complicated by the difficulties in the background subtraction. The source/background beam-switching of the HEXTE clusters (they “rock” periodically to ±3.0° from the source position), is not very efficient for precise background subtraction when the source is located in the densely populated Galactic Center region. There are a number of X-ray sources around XTE J1748–288, namely GX 5-1, GRS 1758–258, GX 3+1 and 1E1740.7–2942 to mention few, each of them luminous enough to affect the results of the background measurement. We have performed a check of the quality of the background subtraction in any given observation by comparing the m-background spectra (the spectra obtained during the -3.0° offset from the source) with the p-background (+3.0° offset). Only observations with an adequate quality of subtraction were accepted for the analysis. Because the rocking planes for clusters A and B are perpendicular to each other, different sky regions are within the field of view of these clusters during the background measurements. Therefore A clusters can provide more accurate background measurements for some observations, and B clusters - for others. After the 8-th observation, when the source flux in the 20–100 keV energy band had dropped below ∼10 cnts/s/cluster, the accuracy of our knowledge of the background became comparable to the source flux, and we excluded these later HEXTE data from our spectral analysis. However, we present the HEXTE observations of the source in its LS in Fig.3. The spectrum plotted there was obtained from carefully selected data, but still should be treated with care.

3 RESULTS

3.1 Energy spectra approximation

We generated the energy spectra of XTE J1748-288 averaging the data over the whole single observations. To trace the evolution of the spectral parameters within some observations, an additional analysis of the spectra, accumulated in 256 sec time intervals, was performed. These spectra were then used to study the correlation of the spectral and variability parameters (see section 3.4).

For the spectral approximation of the first 15 observations we used the model consisted of a multicolor disk blackbody emission component (Shakura & Sunyaev 1973; Mitsuda et al. 1984), a power law component and low energy absorption.

Overall spectral shape for the remaining observations (16–23) can be approximated by power law with low energy absorption. However, strong emission line-like feature around ∼6.5 keV cannot be ignored. This feature may be approximated reasonably well by a Gaussian with centroid energy $E \sim 6.5$ keV and width $\sigma \sim 0.3$ keV. Its absolute intensity appeared to be stable against a decrease of X-ray continuum by a factor of ∼4, thus we believe that this line emission originates from the diffuse X-ray source near the Center of the Galaxy rather than from XTE J1748-288 itself. The measured intensity of this feature, $\sim 3 \times 10^{-3}$ phot/s/cm^2, is in a reasonable agreement with previous measurements of the diffuse line emission from the Galactic Center (e.g. Yamauchi & Koyama 1993). The inclusion of the most prominent Galactic diffuse lines – 6.4, 6.7, and 6.9 keV – also improves the spectral approximation significantly (the widths of the lines were frozen at 0.1 keV – value comparable with the PCA energy resolution). The best fit line intensities ($\sim 1.3 \times 10^{-3}$ phot/s/cm^2 for 6.4 keV line and $\sim 1.5 \times 10^{-3}$ phot/s/cm^2 for 6.7 keV and 6.9 keV lines together ⋆) were approximately constant within the accuracy of the measurements for all LS observations. The equivalent width of the whole K_α feature increased from ∼300 eV in observation #16 to ∼1.1 keV in observation #23.

Spectral fits revealed the presence of an additional line in the spectrum, with the central energy around 8 keV and an intensity $\sim 2 - 3 \times 10^{-4}$ phot/s/cm^2. Even given the moderate energy resolution of the PCA, the presence of this line is evident both when the Fe K_α complex is fitted by by three narrow lines as described above, and when one fits it by one broader line with central energy ∼6.5 keV instead. The 8 keV line feature is likely a complex of the Fe K_β or/and Ni lines of the hard ($kT \sim 7$ keV) optically thin diffuse plasma emission of the Galactic Center region (Kaneda et al. 1997). Note, that the similar spectral feature was observed in the spectrum of XTE J0421+560/CI Cam (Revnivtsev, Emelyanov & Borozdin 1999), that was likely caused by optically thin plasma thermal emission.

The results of the spectral approximation of the PCA data with the analytical models described above are presented in Table 2. Fig.5 shows an evolution of some best fit parameters with time. A correlation between changes in the soft fraction, the disk temperature and the power-law slope during the first 15 observations (VHS) is clearly seen.

3.2 Power density spectrum

In order to analyze the timing properties of XTE J1748–288, we generated power density spectra (PDS) in the 0.01–250 Hz frequency range (for 2–13 keV energy band) using short stretches of data. The resulting spectra were logarithmically rebinned when necessary to reduce the scatter at high frequencies and normalized to the square of the fractional variability. The white-noise level due to the Poissonian statistics corrected for the dead-time effects was subtracted (Vikhlinin, Gilfanov & Churazov 1994; Zhang et al. 1995). To obtain PDS in the lower frequency band ($\sim 5 \times 10^{-4}$ Hz – ∼0.01 Hz) we used the 16-sec integrated data of *Standard 2* mode, because it allowed us to take into account the influence of the background variation on the PDS, which might be of importance at these frequencies.

To study the evolution of the basic timing and spectral parameters of XTE J1748–288 within the individual observations with a relatively high level of variability we generated power density spectra of the source averaged over 256 s time intervals according to the procedure described above (for the results of this study see section 3.4).

We fitted the power density spectra of the source in the 0.02–150 Hz range to analytic models using the χ^2 minimization technique to quantify their characteristics. For the approximation of the PDS obtained during the first 8 observations, we used the sum of a flat-topped band-limited noise (BLN) component: $P_{BLN}(f) \sim exp(-(f/f_{br})^2))$, where f_{br} – is a characteristic break frequency of the BLN continuum, a power law (PL) component – very low frequency noise (VLFN) and up to three harmonically related Lorentzian groups to describe the QPO features (see explanation below).

Fig.2 presents the data and model fit for one observation (June 10). As is clearly seen from the inset of this figure, an approximation of the 20–30 Hz QPO features by a single Lorentzian component does not provide an acceptable fit. This fact could be explained in terms of the existence of an additional high frequency shoulder, similar to those observed in Nova Muscae 1991 and GX 339-4 (Belloni et al. 1997). As we demonstrate below

---

⋆ We added the fluxes from these two lines because PCA does not allow us to resolve them reliably

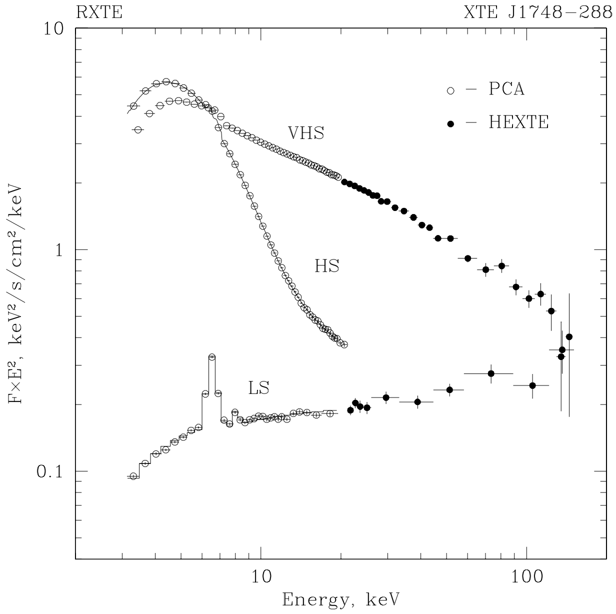

Figure 2. Schematic presentation of the model used for the approximation of the broad-band power density spectra of XTE J1748–288 during the period of maximum luminosity in units f×(rms/mean)^2/Hz (thick solid line). The contributions of the band-limited noise components and the groups of Lorentzian components representing QPO features are shown by long-dashed and dotted lines respectively. The data shown are for the June 10, 1998 observation (PCA data, 2–13 keV energy range). The inset panel demonstrates the difference between the profile of the QPO peak and fit by single Lorentzian component. Inset axis units are the same as for the main panel.

(section 3.4), the QPO centroid frequency derived from the simple Lorentzian fit shifts during the individual observations (Fig.6). Since the strength of the QPO peak is anti-correlated with the QPO centroid frequency, averaging over the whole observation should lead to a steepening of the resulting QPO profile in its low frequency wing and a flattening in its high frequency wing forming a shoulder-like structure. Thus, the appearance of the observed QPO shoulder could be a result of such a displacement of the QPO centroid frequency, for this reason it seems natural to approximate the QPO feature by a sum of several Lorentzians. To obtain a satisfactory fit we used the sum of two Lorentzians for every harmonic. The approximation shows that the frequencies of these additional Lorentzians are also harmonically related which supports our interpretation of the origin of the shoulders.

In observations #9 – 15 the power density spectra were approximated by a power law component, the very low frequency noise (VLFN) component and a Lorentzian profile representing the low frequency QPO.

The best fit parameters of the band limited noise and QPO components are presented in Table 3. QPO rms amplitude is calculated as the quadratic sum of the corresponding rms amplitudes for the Lorentzians used for the QPO approximation. Parameter errors correspond to the 1σ confidence level. These models approximate the data reasonably well, as indicated by the values of reduced χ^2 for the fits.

3.3 Evolution of the source during the outburst

The X-ray flux histories of the XTE J1748-288 outburst based on the *RXTE*/PCA and ASM data in the 3–15 and 15–30 keV energy ranges are shown in Fig.1. The evolution of the source flux in the soft X-ray band (3–15 keV) was characterized by the fast initial rise to a level of ∼600–700 mCrab on a time scale of ∼2–3 days followed by the ∼ 8 day–long maximum and a nearly exponential decay to the quiescent level with e-folding time ∼ 15 days. The flux in the hard band (15–30 keV) undergone a fast initial rise to the ∼300–400 mCrab level followed by the maximum phase of a ∼ 8–day duration and an abrupt decay, which is similar to the behavior of Nova Muscae GS/GRS 1124-683 (Ebisawa et al. 1994) during its outburst of 1991. Based on the results of the spectral and timing analysis, the evolution of XTE J1748–288, in analogy to Nova Muscae 1991, could be divided into three distinct parts, corresponding to three main phenomenological states: *very high* (VHS), *high* (HS) and *low* (LS). At the same time we would like to note, that in the first 8 observations the spectrum of XTE J1748–288 have an extremely bright hard component (the power law component contribution to the total 3–25 keV flux $\gtrsim$80%) which is somewhat different from the usual VHS spectrum. Very similar spectra were observed only with Ginga at the very beginning of the outburst of GS 1124–683 (Kitamoto et al. 1992; Ebisawa et al. 1994), and with Mir-Kvant at the beginning of the outbursts of X-ray Novae KS1730–312 (Borozdin et al. 1995; Trudolyubov et al. 1996) and GRS 1739–278 (Borozdin et al. 1998), but observations of XTE J1748–288 outburst provided an unique opportunity to study this unusually hard VHS spectrum in detail. It is also worth mentioning that contrary to many previous observations of the VHS, which could be distinguished from the HS according to the difference in the power spectrum only, in our case both the energy spectrum and power spectrum in VHS were distinctly different from those in the HS.

Very High State During the first eight RXTE pointed observations (June 4 – 11, 1998) the source was found in an extremely bright state. The broad-band 3–150 keV energy spectrum of XTE J1748–288 in this state can be satisfactorily described by the sum of two components: a relatively weak soft thermal component (contributing only ∼ 10–20 per cent to the total X-ray flux in the 3–25 keV energy band) with a characteristic temperature of ∼ 0.8–1.4 keV and a strong hard component, which is approximately a power law shape and does not show the evidence of a high energy cut-off up to ∼ 150 keV [†]. The corresponding luminosity in the 3–25 keV band uncorrected for the interstellar absorp-

---

[†] An averaged broad-band 3–150 keV spectrum of the observations #3–8 is suggestive for the presence of an additional spectral component in the 10–40 keV energy range, which can be fitted by the Compton reflection (from the neutral medium) model with the reflection parameter $\Omega/2\pi \sim 0.2$. The presence of this component is not required if one analyses the PCA and HEXTE data separately. The cross-calibration uncertainties between the two

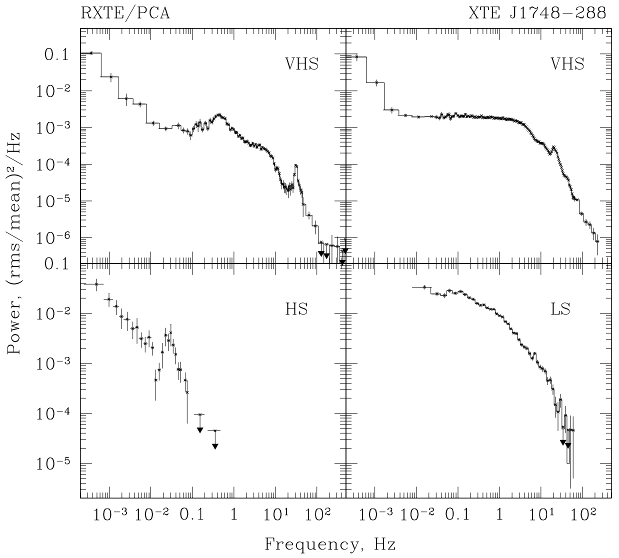

Figure 3. Typical broad-band energy spectra of XTE J1748–288 during the different stages of the 1998 outburst: *VHS* – observation #4, *HS* – observation #10 and *LS* – (observation #20). Hollow and filled circles represent the data of PCA and HEXTE instruments respectively.

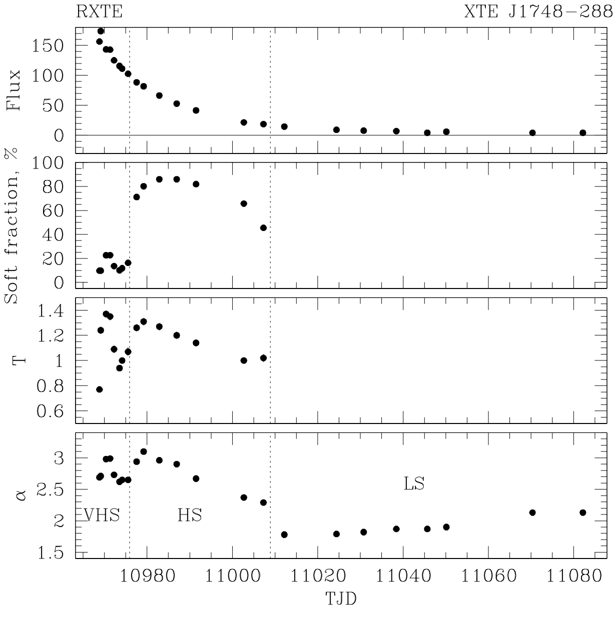

Figure 4. Typical broad-band power density spectra of XTE J1748–288 for different spectral states of the source: *VHS* – averaged observations #3–4 (upper lest panel), *VHS* – averaged observations #5–8 (upper right panel), *HS* – averaged observations #9–15 (left lower panel) and *LS* – averaged observations #16–20 (right lower panel). PCA data for 2 – 13 keV energy band.

tion was at a level of 1–1.5$\times10^{38}$ ergs/s (assuming a 8 kpc distance) during this period.

The broad-band power density spectrum (PDS) of the source is formed by the dominating band-limited noise component (corresponding rms amplitude $\sim$ 5–9 %), the strong QPO feature with centroid frequency $\sim$ 20–30 Hz and a very low frequency noise (VLFN) component with a slope ~ -1.5 and rms amplitude $\sim$ 1.0-1.5 % (Fig.4, *upper panels*).

The correlated spectral and timing evolution of the source during this period is of particular interest. The local increase of the contribution of the soft spectral component to the total X-ray flux in observations # 3–4 (June 6 – 7, 1998) was accompanied by a steepening of the hard spectral component and significant changes in the power density spectrum (Table 2, 3. Fig.4, left upper panel), i.e.:

– the increase of the BLN characteristic break frequency and the decrease of its rms amplitude;

– the increase of the QPO centroid frequency from $\sim$ 20 Hz to $\sim$ 30 Hz;

– the appearance of the additional broad QPO feature at $\sim$ 0.5 Hz (Fox & Lewin 1998);

– the notable rise of the VLFN rms amplitude.

Detected correlations between the spectral and timing properties of the source in this state, discussed in more detail below (see §3.4), holds a wide range of the time scales from seconds to several days.

The two-component spectrum, consisting of the soft thermal component and a hard power law component is a signature of the *high* spectral state of the Galactic black hole candidates (see Tanaka & Shibazaki 1996, and references therein). The *very high* state differs from *high* state mostly by the much stronger fast variability, while the differences in energy spectra are not significant and no good criterium was suggested to distinguish between these two states on spectral ground. In case of XTE J1748-288 the spectrum was sufficiently different from the typical spectra observed previously in the HS and the VHS, because power law component dominated in the 3–25 keV energy band. Fast variability and shape of power spectrum was typical for the VHS of Galactic black hole binaries (e.g. Belloni et al. 1997).

High State . As the flux of XTE J1748–288 dropped below ∼4200 cnts/s/PCA (observations #9–#15), the spectral and timing properties of the source changed drastically. The strength of the hard component in the energy spectrum decreased rapidly and the contribution of the soft thermal component to the total luminosity in the 3–25 keV energy range increased to more than 60 per cent as typical for HS (Fig.3, 5; Table 2).

Simultaneously the shape of the power density spectrum changed qualitatively. The band-limited noise (BLN) component and the high frequency 20–30 Hz QPOs became undetectable, and the amplitude of the fractional variability decreased from ∼10 to ∼1 per cent. The power density spectrum during this period was composed of the power law component with a slope of –1.0–1.5 and a broad QPO peak at ∼0.03 Hz (see Fig.3,5; Table 3).

Low State . The subsequent decline in the intensity of the XTE J1748–288 X-ray flux was accompanied by a gradual decrease of the strength of the soft spectral component (Table 2) and in 16th observation (July 18, 1998) the source was found already in the standard LS. It should be noted that in this state the source flux was

---

instruments do not allow us to state conclusively regarding the presence of this component in the spectrum

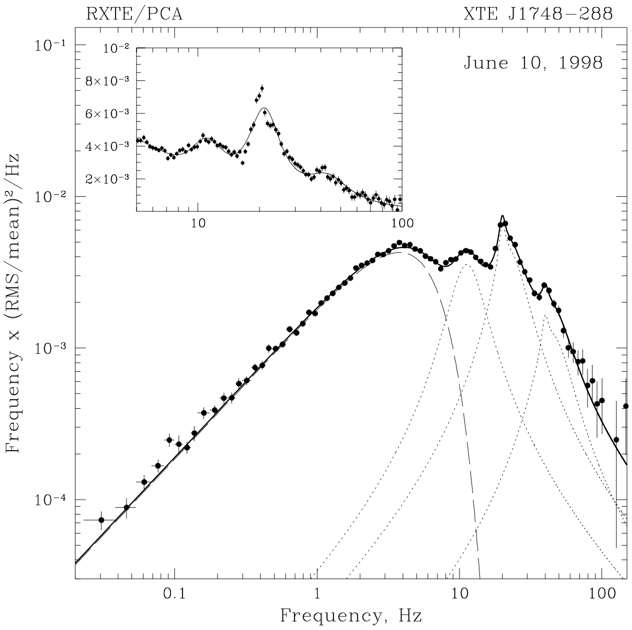

Figure 5. The evolution of the spectral parameters of multicolor blackbody disk plus the power law model for the XTE J1748–288 observations. The soft fraction denotes the ratio of the flux of the soft component to the total flux from the source in energy band 3–25 keV. The dotted lines on the panels denote the approximate time of spectral transitions.

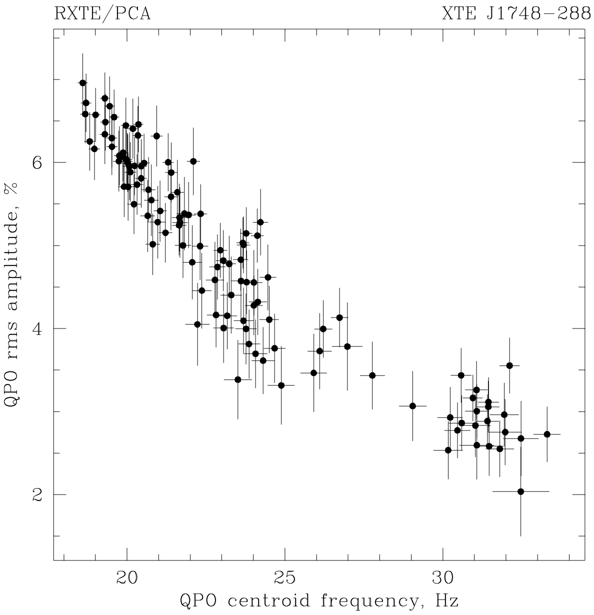

Figure 6. The dependence of the rms amplitude of the high frequency QPO peak on its centroid frequency in the VHS observations (June 4 – June 11, 1998; PCA data). Each point corresponds to the data averaged over 256 sec time intervals.

extremely weak and a substantial part of the observed emission in the PCA energy band can be attributed to the galactic diffuse and point sources, in particular to Sgr B2 (the offset from XTE J1748–288 $\sim12'$).

The *low* state X-ray spectrum in the 3–25 keV energy band was composed by a power law component with a photon index of $\alpha\ \sim2$, a complex of strong emission lines (around 6.5 keV and at $\sim$8 keV) and low energy absorption. The absolute intensity of the lines appeared to be very stable against the decrease of X-ray continuum, which strongly supports the interpretation that they originate from some of the sources within the field of view, but not from the XTE J1748–288. We have performed an additional study to get an estimation for the intensity of the emission line attributed to the XTE J1748–288 itself, assuming the centroid energy of the intrinsic source line to be equal to 6.4 keV. Using the fact that the strong decline in the continuum flux did not result in the statistically significant change in the observed 6.4 keV line flux, we obtained 2σ upper limit $\sim$80 eV on the equivalent width of the intrinsic emission line.

3.4 Correlations between spectral and variability parameters in the very high state

The significant evolution of the spectral and temporal properties of XTE J1748–288 in the VHS provides an excellent opportunity to study their mutual relationship in a wide range of time scales from seconds to several days. In the course of our extended timing analysis the general correlation between the main parameters describing the power density spectrum of the source (QPO centroid frequency, characteristic break frequency of the BLN component, BLN rms, QPO rms) was observed. The dependence of the rms amplitude of main QPO peak on its centroid frequency is shown in Fig.6 . The plot demonstrates evident anticorrelation between these two parameters. Other PDS parameters also appeared to be strongly inter-correlated.

Most striking is the established close relation between the evolution of the spectral and timing parameters of the source. The change of the QPO centroid frequency is correlated with change of the spectral parameters, derived from the energy spectra fits. In particular, there is a clear trend of increasing the QPO centroid frequency with rise of the soft component flux (Fig.7). It should be noted that this type of correlation holds on the wide range of time scales (from seconds to several days).

A similar type of the correlation between the QPO parameters and X-ray flux has also been reported for other Galactic superluminal jet source GRS 1915+105 (Trudolyubov, Churazov & Gilfanov 1999; Markwardt, Swank & Taam 1999), X-ray Nova XTE J1550–564 (Cui et al. 1999), and XTE J1806–246, that is suspected to be a system containing a neutron star (Revnivtsev, Borozdin & Emelyanov 1999). As in the cases of GRS 1915+105 and XTE J1550–564 the QPO peak in the power density spectrum of XTE J1748–288 was detected only in observations characterized by the domination of the hard spectral component. This fact hints on the direct link between the processes of QPO and hard spectral component formation.

Table 2. Spectral parameters of XTE J1748–288, derived using the combination of the multicolor disc blackbody (Mitsuda et al. 1984) and power law models with correction to the interstellar absorption. For the low state observations a power law approximation was used. Parameter errors correspond to 1σ confidence level.

#	T_d keV	$R_{eff}\sqrt{cos\ i}\ D_{10}{}^*$ km	α_{pl} ph. index	N_H $10^{22}\ cm^{-2}$	Flux (3–25 keV) $\times 10^{-10}$ ergs/s/cm^2	Flux$_{\rm soft}$(3-25 keV) $\times 10^{-10}$ ergs/s/cm^2	χ^2(46 dof)
			Very High State				
1	0.77 ± 0.02	55.29 ± 1.11	2.69 ± 0.03	10.9 ± 2.1	156.4 ± 4.7	15.2 ± 0.3	29.54
2	1.24 ± 0.03	11.95 ± 0.89	2.71 ± 0.03	8.17 ± 0.8	173.8 ± 5.3	16.9 ± 0.5	34.08
3	1.37 ± 0.03	13.17 ± 0.26	2.98 ± 0.03	10.4 ± 0.3	143.2 ± 4.3	32.3 ± 0.4	29.24
4	1.35 ± 0.03	13.47 ± 0.27	2.99 ± 0.03	10.1 ± 0.3	142.8 ± 4.3	32.4 ± 1.0	26.97
5	1.09 ± 0.03	17.65 ± 0.35	2.73 ± 0.03	9.3 ± 0.3	125.0 ± 3.8	17.0 ± 1.0	28.83
6	0.94 ± 0.02	23.27 ± 0.47	2.62 ± 0.03	9.3 ± 0.4	115.6 ± 3.5	11.7 ± 0.5	31.26
7	1.00 ± 0.02	20.44 ± 0.41	2.65 ± 0.03	9.1 ± 0.3	111.2 ± 3.3	13.1 ± 0.4	25.95
8	1.07 ± 0.03	17.93 ± 0.36	2.65 ± 0.03	7.3 ± 0.3	102.6 ± 3.1	16.7 ± 0.4	16.68
			High State				
9	1.26 ± 0.03	21.27 ± 0.43	2.94 ± 0.03	6.8 ± 0.2	88.4 ± 2.7	62.9 ± 0.5	26.63
10	1.31 ± 0.03	19.92 ± 0.40	3.10 ± 0.03	7.8 ± 0.3	81.8 ± 2.5	65.6 ± 1.9	30.54
11	1.27 ± 0.03	20.39 ± 0.41	2.96 ± 0.03	7.5 ± 0.2	66.5 ± 2.0	57.2 ± 2.0	24.35
12	1.20 ± 0.03	21.07 ± 0.42	2.90 ± 0.03	7.4 ± 0.2	52.9 ± 1.6	45.5 ± 1.7	31.80
13	1.14 ± 0.03	21.08 ± 0.42	2.67 ± 0.03	7.4 ± 0.2	41.5 ± 1.2	34.0 ± 1.4	30.40
14	1.00 ± 0.02	20.05 ± 0.40	2.37 ± 0.03	6.8 ± 0.3	21.6 ± 0.6	14.2 ± 1.0	34.94
15	1.02 ± 0.03	13.95 ± 0.28	2.29 ± 0.03	5.7 ± 0.3	18.7 ± 0.6	8.5 ± 0.4	36.11
			Low State				
16			1.78 ± 0.02	3.4 ± 0.4	14.6 ± 0.7		32.2
17			1.79 ± 0.02	4.9 ± 0.5	9.2 ± 0.6		47.0
18			1.82 ± 0.02	5.0 ± 0.2	7.8 ± 0.5		33.1
19			1.87 ± 0.02	5.8 ± 0.3	7.0 ± 0.4		30.6
20			1.87 ± 0.02	5.8 ± 0.2	4.2 ± 0.3		28.1
21			1.90 ± 0.02	5.2 ± 0.5	6.0 ± 0.3		53.5
22			2.13 ± 0.02	7.3 ± 0.4	4.2 ± 0.2		48.6
23			2.13 ± 0.02	7.0 ± 0.5	4.1 ± 0.1		51.3

*–D_{10} – source distance in units of 10 kpc. i – inclination angle of the system

4 DISCUSSION

Many bright X-ray transients are reputed black hole candidates and demonstrate similar X-ray spectra and fast variability. During the outburst these systems are typically found in one of two qualitatively distinguishable spectral states: in the *high* state composed of the bright thermal component and the extended hard power-law, or in the *low* state with the hard power-law spectrum with a photon index of ~1.5 and an exponential high energy cutoff. A more detailed description of these states can be found elsewhere (Sunyaev et al. 1994; Tanaka & Lewin 1995; Tanaka & Shibazaki 1996). A third, *very high*, state has been recognized also, with two component spectrum similar to the HS, but with somewhat stronger power-law component and with much stronger fast variability (Miyamoto et al. 1991, 1994; Takizawa et al. 1997). The spectral evolution of X-ray transients is usually in correlation with X-ray flux changes, so it is widely believed that state transitions are driven by the variable accretion rate. Such transitions were also observed in the persistent black hole systems, namely, Cyg X-1 and GX 339-4, but the dynamics of these systems is much slower, so they are more often observed in one of these states and typically switch to another state once every several years (Sunyaev & Truemper 1979; Makishima et al. 1986; Cui et al. 1998; Dove et al. 1998; Trudolyubov et al. 1998).

The transient X-ray source XTE J1748–288 resembles other black hole X-ray transients in many ways. The general properties of the source light curves are similar to the properties of the light curves of black hole X-ray Novae such as A 0620-00, GS 2000+25, GS/GRS 1124-68, GRS 1009-45, GRS1739-278 and others (see Chen, Shrader & Livio 1997 for review, and references therein). During the 1998 outburst the source was observed by *RXTE* in *very high*, *high* and *low* spectral states, which are very typical for black hole systems. During several observations corresponding to the peak X-ray flux, the spectrum of the source was in an unusual VHS, a very bright hard component was observed. Similar spectra were detected at the beginning of the outbursts of X-ray black hole Novae GS/GRS1124–68 (Ebisawa et al. 1994; Miyamoto et al. 1994), KS/GRS 1730–312 (Borozdin et al. 1995; Trudolyubov et al. 1996) and GRS 1739–278 (Borozdin et al. 1998). Here we studied this spectrum in more detail.

The transition of XTE J1748–288 from the *very high* state to the *high* state changed both the spectral and fast variability properties of the X-ray flux of XTE J1748–288. Unlike the case of Nova Muscae (Miyamoto et al. 1994; Ebisawa et al. 1994), hard component dom-

Table 3. The characteristics of the power density spectra of XTE J1748–288. Parameter errors correspond to 1σ confidence level. rms_{total}, and rms_{BLN} represent total rms amplitude and total rms amplitude of the band-limited noise (BLN) component integrated over $0.02-150$ Hz frequency range, f^{br}_{BLN} and f_{QPO} represent the characteristic break frequency of the BLN component and the QPO centroid frequency. rms^1_{QPO}, $\mathrm{rms}^{1/2}_{QPO}$ and rms^2_{QPO} are the rms amplitudes of the groups of Loretzians used to approximate the first (fundamental) harmonic, subharmonic and second harmonic of the QPO. $\mathrm{f}^{shoulder}_{QPO}$ represents the centroid frequency of the accompanying Lorentzian (see text)

#	$\mathrm{rms_{total}}$	$\mathrm{f^{br}_{BLN}}$, Hz	$\mathrm{rms_{BLN}}$	$\mathrm{f_{QPO}}$, Hz	$\mathrm{f^{shoulder}_{QPO}}$	$\mathrm{rms^1_{QPO}}$	$\mathrm{rms^{1/2}_{QPO}}$	$\mathrm{rms^2_{QPO}}$	χ^2(dof)
				Very High state (2–13 keV, 0.02–150 Hz)					
2	11.7 ± 0.3	3.79 ± 0.32	8.69 ± 0.71	21.8 ± 0.5	-	5.8 ± 0.9	4.7 ± 0.9	-	33(36)*
3	7.4 ± 0.1	6.14 ± 0.14	5.15 ± 0.16	31.6 ± 0.2	-	3.2 ± 0.1	-	-	228(183)
				0.48 ± 0.02		2.7 ± 0.2			
4	7.1 ± 0.1	6.15 ± 0.13	4.83 ± 0.14	31.3 ± 0.2	-	3.1 ± 0.2	-	-	229(183)
				0.44 ± 0.02		2.9 ± 0.2			
5	12.1 ± 0.1	4.27 ± 0.05	8.80 ± 0.11	23.7 ± 0.1	24.8 ± 0.2	5.4 ± 0.3	5.0 ± 0.2	2.5 ± 0.4	217(177)
6	13.2 ± 0.1	3.68 ± 0.04	8.95 ± 0.09	20.2 ± 0.1	21.3 ± 0.1	6.6 ± 0.3	5.6 ± 0.1	3.3 ± 0.3	208(177)
7	13.1 ± 0.1	3.79 ± 0.03	9.04 ± 0.05	20.0 ± 0.1	21.5 ± 0.1	6.3 ± 0.3	5.5 ± 0.1	3.3 ± 0.3	209(177)
8	12.4 ± 0.1	4.10 ± 0.04	8.91 ± 0.11	22.6 ± 0.2	24.1 ± 0.2	5.5 ± 0.3	5.2 ± 0.2	3.0 ± 0.3	188(177)
				High state (2-13 keV, 5×10^{-4}–0.2 Hz)					
		α_{VLFN}	$\mathrm{rms_{VLFN}}$,%	$\mathrm{f_{QPO}}$, Hz	FWHM, Hz	$\mathrm{rms_{QPO}}$,%			χ^2(dof)
9–15		-1.14 ± 0.08	0.86 ± 0.09	$(2.9 \pm 0.1) \times 10^{-2}$	$(1.1 \pm 0.4) \times 10^{-2}$	0.77 ± 0.14			21.1(24)

– all *rms* values in %

* – this power density spectrum was obtained in the frequency range 0.3–50 Hz (slew part of the observation with total exposure 64 sec)

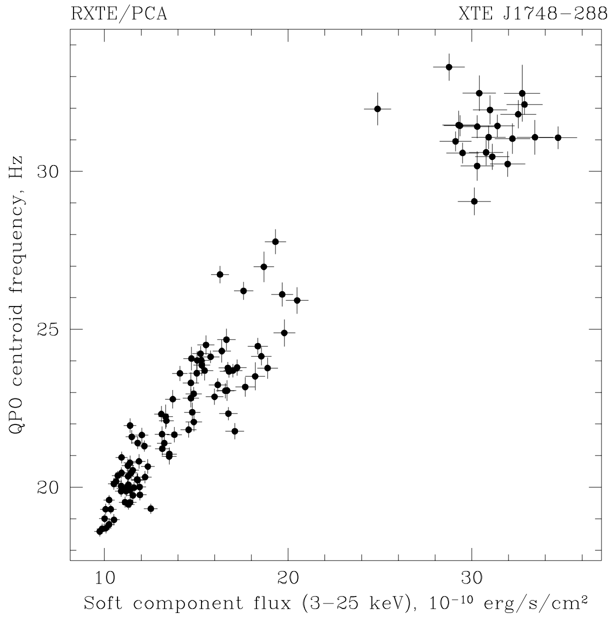

Figure 7. The dependence of the QPO centroid frequency on the X-ray flux in the soft spectral component in the 3–25 keV energy range (without correction for an interstellar absorption). The parameters of the soft component are for the best-fit approximation by multicolor disk black body plus power law model. PCA data for the VHS observations (June 4–11, 1998) have been used. Each point corresponds to the data averaged over 256-sec time intervals.

inated spectrum during all VHS observations. The soft component in the spectrum of the XTE J1748–288 increased rapidly by a factor of ~4 after the transition, while the total flux in the energy band 3–25 keV continued to decrease smoothly. The amplitude of the fast variability dropped down during the transition and PDS shape changed qualitatively (see Fig.4). PDS of the source X-ray flux in the HS has a power law shape of the continuum and shows the presence of the low-frequency QPO peak at ~ 0.029 Hz, resembling the properties of the *high* state PDS of the well-known black hole candidate LMC X-1 (its form was described by the sum of the power law component and a QPO peak with a centroid frequency of ~ 0.075 Hz) (Ebisawa et al. 1989).

After the subsequent decrease of the luminosity, the XTE J1748–288 switched the source to the *low* state typical for the black hole X-ray Novae at this stage of the outburst evolution.

The shape of the broad-band power density spectrum of XTE J1748–288 in the VHS was similar to the PDS observed for the Galactic black hole candidates GX 339-4, Nova Muscae 1991 and GRS 1915+105 (Miyamoto et al. 1994; Belloni et al. 1997; Trudolyubov, Churazov & Gilfanov 1999): it was dominated by a strong band-limited noise with QPO components.

The correlated spectral and timing evolution of the source during the VHS and, in particular, the observed trend of increasing the QPO centroid frequency with the rise of the soft component flux on the wide range of time scales is of special importance. A similar type of correlation between the QPO parameters and X-ray flux have also been reported for other Galactic black hole candidates: GRS 1915+105 and XTE J1550–564 (Trudolyubov, Churazov & Gilfanov 1999; Markwardt, Swank & Taam 1999; Cui et al. 1999), which hints at the general mechanism of the X-ray emission generation for this class of objects.

One of the possible and probably the most promising way to explain these observational results for black hole systems is to use the models based on the idea of a shock front formation between two distinct parts of the accretion flow producing the bulk of X-rays: the central region responsible for the generation of the hard spectral component and optically thick accretion disk (Chakrabarti & Titarchuk 1995). The oscillations in shock geometrical parameters (i.e. height, width) may modulate the flux of the "seed" photons from the inner boundary of the optically thick accretion disk and change the state of matter in the optically thin region - and as a result, QPOs of X-ray flux are to be detected (Titarchuk, Lapidus & Muslimov 1998; Molteni, Sponholz & Chakrabarti, 1996). In this case the time scale of the oscillations is determined by the position of the boundary between the optically thick and thin regions, which in turn is directly related to the luminosities of the soft and hard spectral components. Hence the observed correlation between the QPO frequency and X-ray flux could be naturally explained in the framework of this model.

The observed complex of the general spectral and timing properties of XTE J1748–288 is similar to that of the dynamically proven black hole X-ray Novae and Galactic superluminal jet sources. This fact could hint at the universal character of evolution of the accretion flow in the black hole systems and its direct link to the mechanism of the formation of relativistic ejections of matter.

ACKNOWLEDGMENTS

This research has made use of data obtained through the High Energy Astrophysics Science Archive Research Center Online Service, provided by the NASA/Goddard Space Flight Center.

The authors wish to thank Dr.M.Gilfanov for his valuable suggestions, which helped us to improve the paper significantly. We are grateful to M.N.R.A.S. anonymous referee for his/her helpful comments, and to Ms. Kate O'Shea for the language editoring of the manuscript. Part of this work was supported by RBRF 96-02-18588 and INTAS 93-3364-ext grants.

REFERENCES

Belloni T., van der Klis, M., Lewin W. H. G., van Paradijs J., Dotani T., Mitsuda K., Miyamoto S., 1997, A&A, 332, 857

Borozdin K. N., Aleksandrovich N. L., Arefiev V. A., Sunyaev R. A., Skinner G. K., 1995, Astr.L. 21, 212

Borozdin K. N., Revnivtsev M. G., Trudolyubov S. P., Aleksandrovich N. L., Sunyaev R. A., Skinner G. K., 1998, Astr.L. 24, 435

Borozdin K., Revnivtsev M., Trudolyubov S., Shrader C., Titarchuk L., 1999, ApJ, accepted (astro-ph/9812442)

Chakrabarti S. K., Titarchuk L. G., 1995, ApJ, 452, 226

Chen W., Shrader C. R., Livio M., 1997, ApJ, 491, 312

Cui W., Ebisawa K., Dotani T., Kubota A., 1998, ApJ, 493, L75

Cui W., Zhang S. N., Chen W., Morgan E. H., 1999, ApJ, in press (astro-ph/9812308)

Dove J. B., Wilms J., Nowak M. A., Vaughan B. A., Begelman M. C., 1998, MNRAS, 298, 729

Ebisawa K., Mitsuda K., Inoue H., 1989, PASJ, 41, 519

Ebisawa K., Ogawa M., Aoki T., Dotani T., Takizawa M., Tanaka Y., Yoshida K., Miyamoto S., Iga S., Hayashida K., Kitamoto S., Terada K., 1994, PASJ, 46, 375

Fender R. P., Stappers B. W., 1998, IAU Circ. 6937

Fox D., Lewin W., 1998, IAU Circ. 6964

Hjellming R. M., Rupen M. P., Mioduszewski A. J., 1998, IAU Circ. 6934

Hjellming R. M., Rupen M. P., Chigo F., Waltman E. B., Mioduszewski A. J., 1998a, IAU Circ. 6937

Hjellming R. M., Rupen M. P., Mioduszewski A. J., Smith D. A., Harmon B. A., Waltman E. B., Chigo F. D., Pooley G. G., 1998b, American Astron.Soc.Meeting #193, 103.08

Kaneda H., Makishima K., Yamauchi S., Koyama K., Matsuzaki K., Yamasaki N. Y., 1997, ApJ, 491, 638

Kitamoto S., Tsunemi H., Miyamoto S., Hayashida K., 1992, ApJ, 394, 609

Makishima K., Maejima Y., Mitsuda K., Brandt H. V., Remillard R. A., Tuohy I. R., Hoshi R., Nakagawa M., 1986, ApJ, 308, 635

Markwardt C. B., Swank J. H., Taam R. E., 1999, ApJ, in press (astro-ph/9901050)

Mitsuda K., Inoue H., Koyama K., Makishima K., Matsuoka M., Ogawara Y., Suzuki K., Tanaka Y., Shibazaki N., Hirano T., 1984, PASJ, 36, 741

Miyamoto S., Kimura K., Kitamoto S., Dotani T., Ebisawa K., 1991, ApJ, 383, 784

Miyamoto S., Kitamoto S., Iga S., Hayashida K., Terada K., 1994, ApJ, 435, 398

Molteni D., Sponholz H., Chakrabarti S. K., 1996, ApJ, 457, 805

Revnivtsev M. G., Emelyanov A. N., Borozdin K. N., 1999, Astr.L., 25, 350 (astro-ph/9810156)

Revnivtsev M. G., Borozdin K. N., Emelyanov A. N., 1999, A&AL, 334, 25

Rupen M. P., Hjellming R. M., Mioduszewski A. J. 1998, IAU Circ. 8938

Shakura N. I., Sunyaev R. A., 1973, A&A, 24, 337

Smith D. A., Levine A., Wood A., 1998, IAU Circ. 6932

Strohmayer T., Marshall F. E., 1998, IAU Circ. 6934

Sunyaev R. A., Truemper J., 1979, Nat, 279, 506

Sunyaev R. A., Borozdin K. N., Aleksandrovich N. L., Arefiev V. A., Kaniovsky A. S., Efremov V. V., Maisack M., Reppin C., Skinner G. K., 1994, Astr.L., 20, 777

Tanaka Y., Lewin W. H. G., 1995, in X-ray Binaries, ed. W. Lewin, J. van Paradijs, E. van der Heuvel (Cambridge: Cambridge Univ. Press), 126

Tanaka Y., Shibazaki N., 1996, ARAA, 34, 607

Takizawa M., Dotani T., Mitsuda K., Matsuba E., Ogawa M., Aoki T., Asai K., Ebisawa K., Makishima K., Miyamoto S., Iga S., Vaughan B., Rutledge R. E., Lewin W. H. G. 1997, ApJ, 489, 272

Titarchuk L., Lapidus I., Muslimov A., 1998, ApJ, 499, 315

Trudolyubov S. P., Gilfanov M. R., Churazov E. M., Borozdin K. N., Aleksandrovich N. L., Sunyaev R. A., Khavenson N. G., Novikov B. S., Vargas M., Goldwurm A., Paul J., Denis M., Borrel V., Bouchet L., Jourdain E., Roques J.-P., 1996, Astr.L., 22, 664

Trudolyubov S., Gilfanov M., Churazov E., Sunyaev R., Khavenson N., Dyachkov A., Tserenin I., Sukhanov K., Laurent P., Ballet J., Goldoni P., Paul J., Roques J.-P., Borrel V., Bouchet L., Jourdain E., 1998, A&A, 334, 895

Trudolyubov S., Churazov E., Gilfanov M., 1999, Astr.L., in press (astro-ph/9811449)

Vikhlinin A., Gilfanov M., Churazov E., 1994, A&A, 287, 73

Yamauchi S., Koyama K., 1993, ApJ, 404, 620

Zhang W., Jahoda K., Swank J. H., Morgan E. H., Giles A. B., 1995, ApJ, 449, 930